JOURNAL OF MATERIALS SCIENCE **35** (2000) 1737–1742

# Microstructure and electrical characterisations of K-modified PLZT

S. R. SHANNIGRAHI, R. N. P. CHOUDHARY, H. N. ACHARYA
*Department of Physics and Meteorology, Indian Institute of Technology, Kharagpur-721302, India*

T. P. SINHA
*Department of Physics, Bose Institute, 93/1, Acharya Prafulla Chandra Road, Calcutta-700009, India*
*E-mail: crnpfl@phy.iitkgp.ernet.in*

Potassium-modified PLZT [$Pb_{0.92}(La_{1-z}K_z)_{0.08}(Zr_{0.60}Ti_{0.40})_{0.98+0.04z}O_3$ ($z = 0.0$, 0.1, 0.3, 0.5, 0.7)] ceramics were synthesised using sol-gel technique. Preliminary structural and microstructural parameters were determined using XRD, SEM and TEM techniques. Detailed studies of dielectric properties at 10 kHz in a wide temperature range suggest that the compounds have diffuse phase transition of second order. Studies of spontaneous polarisation, pyroelectric and piezoelectric properties yielded data for devices. 

## 1. Introduction

PZT is a solid-solution of ferroelectric lead titanate ($PbTiO_3$) and antiferroelectric lead zirconate ($PbZrO_3$) with varying degree of composition of the compounds [$Pb(Zr_xTi_{1-x})O_3$ where $0 < x < 1$]. The PZT ceramics with compositions near phase boundary offers good piezoelectric and other properties [1, 2]. It is well established that substitution of $La^{+3}$ at the Pb-site of PZT (abbreviated as PLZT) gives improved piezoelectric and opto-electronic properties of the materials due to the high solubility of La in PZT, reduction of distortion in perovskite structure in PLZT and formation of high-density samples. It is most interesting to observe diffuse phase transition (DPT) in complex PLZT [3–5]. Though some work has been done in the past to study the effect of substitution of single, isovalent, supervalent or subvalent dopants with varying concentration at the Pb- and/or Zr/Ti-sites of the PZT [6–10], very little work on the effect of double doping at the Pb-site have been reported [11]. Therefore, we have studied structural, microstructural, dielectric, piezoelectric, hysteresis and pyroelectric properties of the $Pb_{0.92}(La_{1-z}K_z)_{0.08}(Zr_{0.60}Ti_{0.40})_{0.98+0.04z}O_3$ ($z = 0.0$, 0.1, 0.3, 0.5, 0.7) (PLKZT) system.

## 2. Experimental procedure

$Pb_{0.92}(La_{1-z}K_z)_{0.08}(Zr_{0.60}Ti_{0.40})_{0.98+0.04z}O_3$ ($z = 0.0$, 0.1, 0.3, 0.5, 0.7) (PLKZT) ceramics were synthesised using: lead acetate trihydrate $Pb(CH_3COO)_2 \cdot 3H_2O$ (99.9%, M/s. E. Merck, Germany), lanthanum acetate hexahydrate $La(CH_3COO)_3 \cdot 6H_2O$ (99.9%, M/s. B.D.H., UK), potassium acetate dihydrate $CH_3COOK \cdot 2H_2O$ (98%, M/s. Aldrich, USA), zirconium propoxide $Zr(C_3H_7O)_4$ (70 wt % in 1–propanol, M/s. Fluka, Switzerland) and titanium isopropoxide $Ti[(CH_3)_2CHO]_4$ (>97% Ti content, M/s. E. Merck, Germany) in proper stoichiometry. Glacial acetic acid and distilled water were used as solvents. Ethylene glycol was used as an additive in order to get monolithic gel. All the above acetates were dissolved separately in acetic acid in the ratio of 2 g of salt in 1 ml acid and were heated at 110°C for 30 minutes to remove the water content, and then cooled down to 80°C. These solutions were mixed in a beaker and stirred. During stirring zirconium propoxide followed by titanium isopropoxide were added in the mixture. Ethylene glycol was then added in the proportion of 1 ml to 10 g of lead acetate. After completion of the initial reaction the glycol was added, since residual titanium isopropoxide and zirconium propoxide alcolyze with ethylene glycol to form a condensed solid. A small amount of distilled water was added to get the final sol. The sol was soaked at 60°C for 24 h to get the clear transparent gel. The gel was dried at 100°C for 72 h and a light brown powder was obtained. DTA analysis of the gel powders at different temperatures was done by a thermal analyser (Shimadzu DT–40) to select suitable calcination temperature of PLKZT. The oven dried powdered gels were calcined at 550°C for 15 h. The powders were cold pressed into pellets at a pressure of $6 \times 10^6$ Pa using a hydraulic press. The pellets were then sintered for 60 h at 1200°C. In order to prevent PbO loss of vaporisation during sintering and to maintain the stoichiometry of the compounds, an equilibrium PbO vapour pressure was established with $PbZrO_3$ as setter and placing everything in the covered platinum crucible. The density of the sintered pellet samples was measured by Archemedes' method and was found to be 97–98% of their theoretical value.

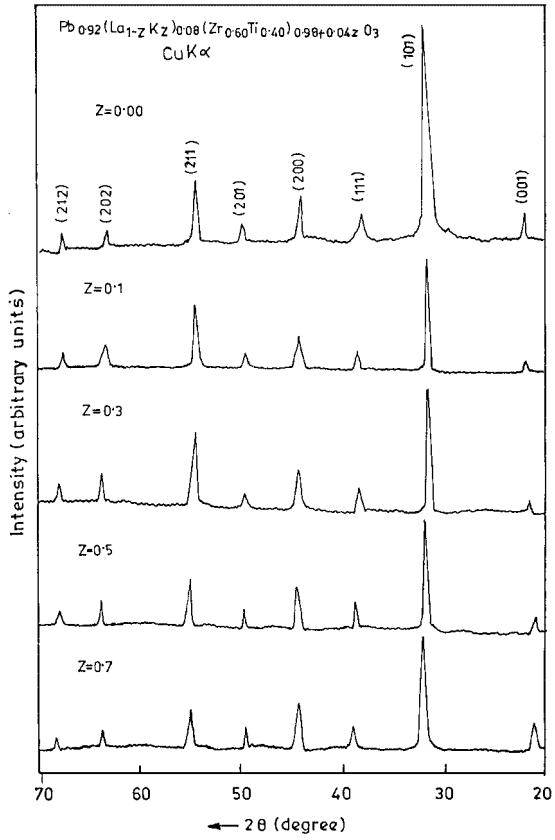


*Figure 1* Comparison of XRD of the PLKZT.

The formation of single phase compounds was checked by X-ray diffraction (XRD) technique with powder diffractometer (Philips PW 1877) using Cu $K_\alpha$ radiation ($\lambda = 0.15418$ nm) in a wide range of Bragg angles ($20^\circ \leq 2\theta \leq 70^\circ$) at room temperature with the scanning rate $3^\circ \text{min}^{-1}$ on powders as well as on sintered pellets.

Measurements of dielectric constant ($\varepsilon$) and tangent loss ($\tan\delta$) of the silver electroded samples were carried out using a GR 1620 AP capacitance measuring assembly with a three-terminal sample holder in a wide temperature range (30–350°C) at 10 kHz.

The microstructures of the samples were analysed by TEM (JEM 200 CX) and SEM (CAMSCAN 180). The temperature variation of remanent polarisation ($P_r$) and coercive field ($E_c$) of the samples were recorded at

TABLE I Comparison of cell parameters ($a$ & $c$), density ($d$), grain size and particle size of PLKZT

| $z$ | 0.0 | 0.1 | 0.3 | 0.5 | 0.7 |
|---|---|---|---|---|---|
| $a$ (Å) | 4.0049 | 4.0221 | 4.0952 | 4.1039 | 4.1303 |
| $c$ (Å) | 4.0102 | 4.0356 | 4.1155 | 4.1329 | 4.1330 |
| $d$ ($\text{g}\cdot\text{cc}^{-1}$) | 7.871 | 7.751 | 7.670 | 7.622 | 7.550 |
| Av. Grain size (SEM) ($\mu$m) | 2.80 | 2.40 | 2.70 | 3.20 | 3.75 |
| Av. Particle size (TEM) (Å) | 120 | 165 | 240 | — | — |

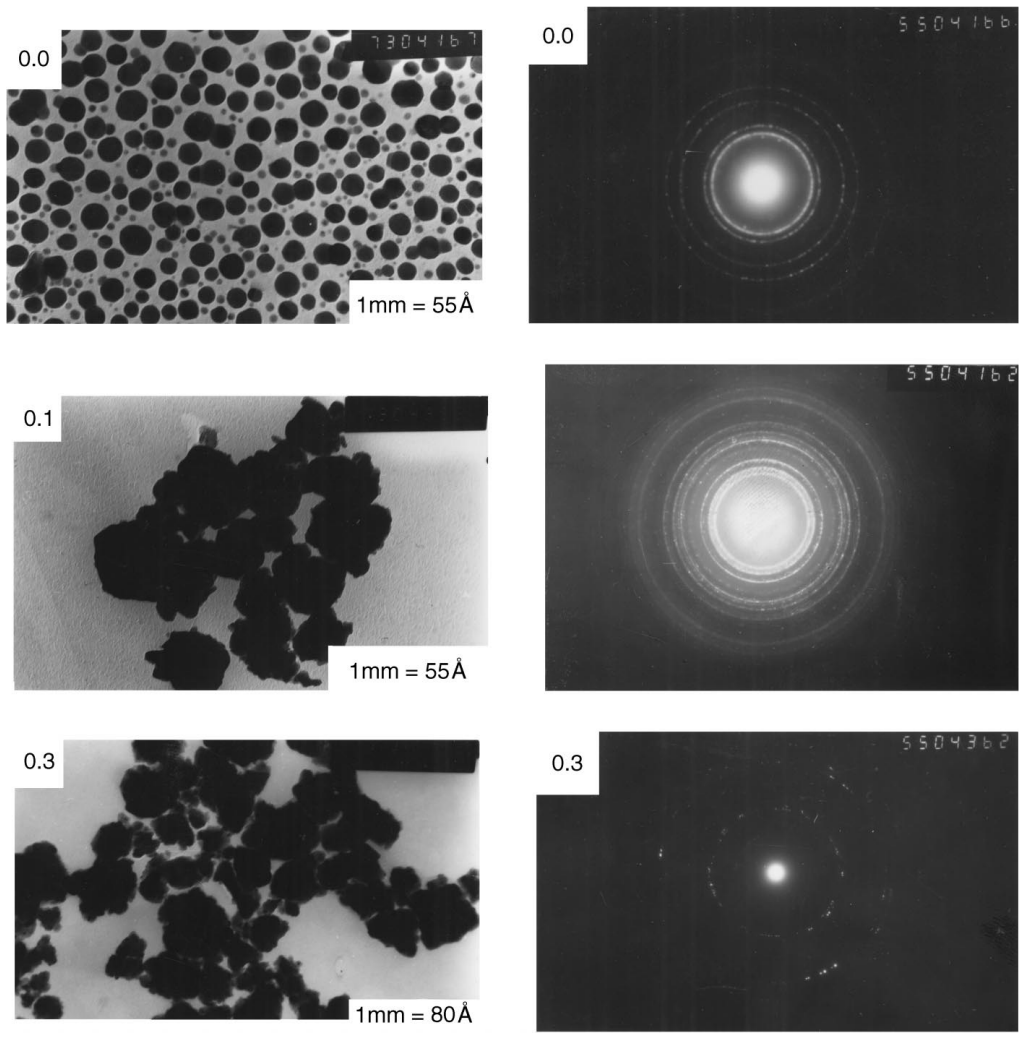


*Figure 2* TEM micrographs and diffraction patterns (inset) of PLKZT for $z =$ 0.0, 0.1, 0.3.

50 Hz with an ac field of 20 kV · cm$^{-1}$ using a dual-trace oscilloscope attached to the modified Sawyer-Tower circuit.

The piezoelectric coefficients and parameters were measured on the poled samples (15 kV · cm$^{-1}$ dc field) using HP 4194A Impedance/Gain Phase Analyser and Berlincourt $d_{33}$ meter.

Measurement of pyroelectric coefficient was performed on the poled samples using laboratory fabricated experimental set-up with temperature sweep rate of 2°C · min$^{-1}$.

## 3. Results and discussion

The room temperature XRD patterns of the calcined powders and sintered pellets of PLKZT samples were found similar. All the XRD peaks were indexed and calculated lattice parameters were refined using least-squares method of computer package "PowdMult". It is found that the crystal structure of PLZT is not affected by the substitutions of the $K^+$ ions even upto 7 mole% (Fig. 1). However, a small change in the lattice parameters was found (Table I). All the $K^+$ doped PLZT compounds have tetragonal structure at room

TABLE II Comparison of some observed interplanar spacing (Å) measured from XRD and TEM of PLKZT, with observed intensities in parenthesis

| $z$ | 0.0 | | 0.1 | | 0.3 | | 0.5 | 0.7 |
|---|---|---|---|---|---|---|---|---|
| $hkl$ | $d_{XRD}$ | $d_{TEM}$ | $d_{XRD}$ | $d_{TEM}$ | $d_{XRD}$ | $d_{TEM}$ | $d_{XRD}$ | $d_{XRD}$ |
| 001 | 4.005(15) | — | 4.036(8) | — | 4.116(10) | — | 4.133(13) | 4.133(21) |
| 101 | 2.834(100) | — | 2.849(100) | — | 2.903(100) | — | 2.912(100) | 2.921(100) |
| 111 | 2.314(12) | 2.312 | 2.325(17) | 2.323 | 2.368(20) | 2.371 | 2.374(15) | 2.386(12) |
| 200 | 2.003(16) | 2.007 | 2.011(33) | — | 2.048(33) | 2.049 | 2.053(21) | 2.067(43) |
| 201 | 1.793(5) | — | 1.799(14) | — | 1.833(14) | — | 1.838(9) | 1.841(11) |
| 211 | 1.637(23) | — | 1.643(58) | 1.642 | 1.673(56) | — | 1.672(32) | 1.681(28) |
| 220 | 1.418(24) | 1.413 | 1.422(18) | — | 1.448(22) | — | 1.451(20) | 1.462(19) |
| 221 | 1.336(8) | 1.310 | 1.341(9) | 1.346 | 1.366(7) | 1.364 | 1.370(9) | 1.379(7) |

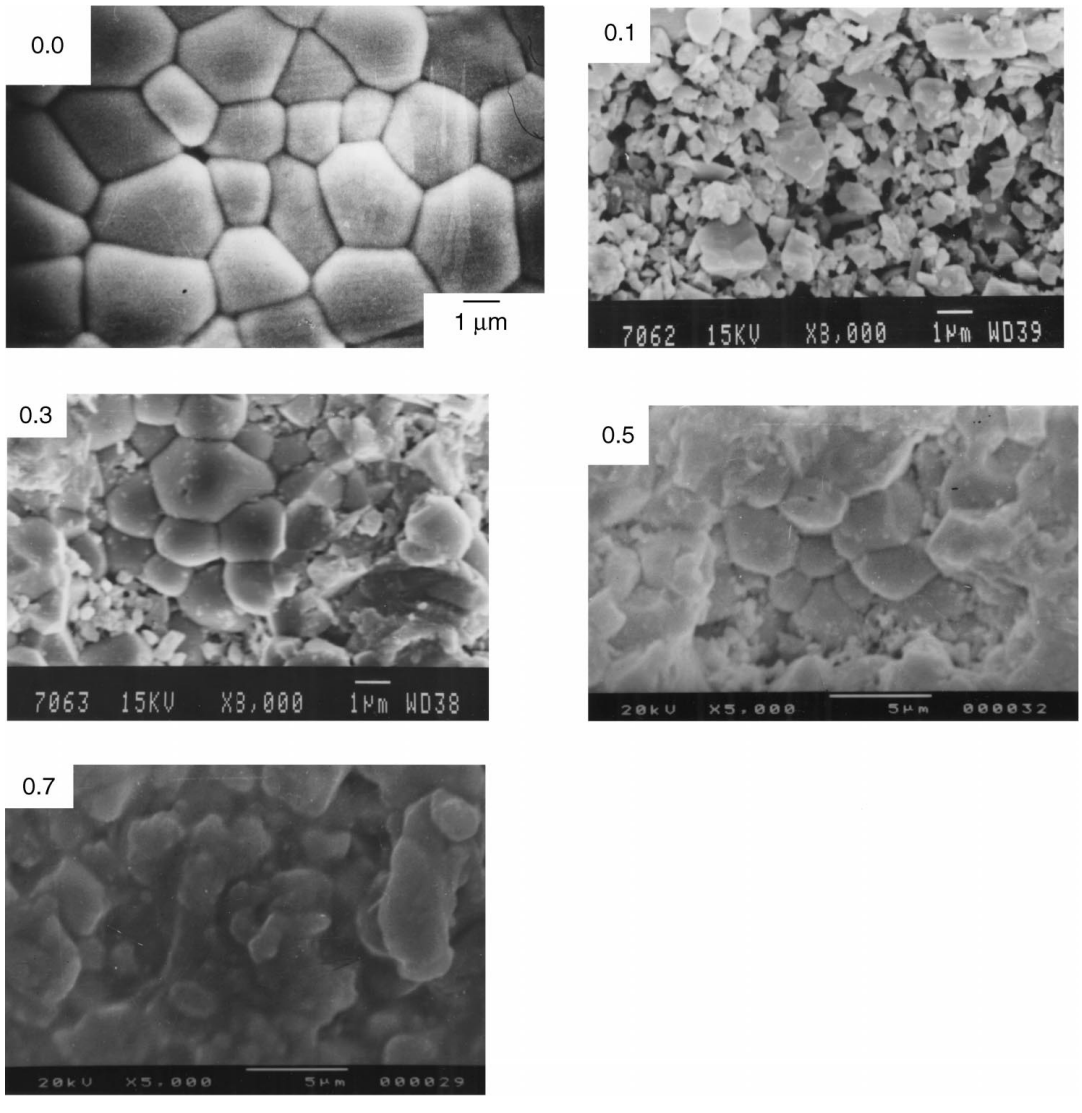


*Figure 3* SEM micrographs of PLKZT for $z = 0.0$, 0.1, 0.3, 0.5 and 0.7.

TABLE III Comparison of dielectric, hysteresis, pyroelectric and piezoelectric parameters of PLKZT

| $z$ | 0.0 | 0.1 | 0.3 | 0.5 | 0.7 |
|---|---|---|---|---|---|
| Diffusivity ($\gamma$) | 1.72 | 1.75 | 1.88 | 1.96 | 1.84 |
| Activation energy $E_a$ (eV) | 0.90 | 0.31 | 0.45 | 0.52 | 0.88 |
| $P_r$ ($\mu C \cdot cm^{-2}$) | 17.90 | 16.10 | 18.65 | 21.21 | 24.40 |
| $E_c$ ($kV \cdot cm^{-1}$) | 6.5 | 5.76 | 6.25 | 6.88 | 7.75 |
| $P^T$ at $T_c$ ($nC \cdot cm^{-2} \cdot {}^\circ C^{-1}$) | 126.2 | 65.4 | 77.8 | 94.3 | 110 |
| $d_{33}$ ($10^{-12}$ $C \cdot N^{-1}$) | 569 | 492 | 388 | 340 | 284 |
| $k_p$ | 0.54 | 0.39 | 0.41 | 0.25 | 0.32 |
| $Q_m$ | 421 | 317 | 305 | 280 | 188 |
| $k_{31}$ | 0.10 | 0.15 | 0.38 | 0.23 | 0.19 |
| FC (kHz. m) | 0.66 | 0.88 | 1.03 | 1.01 | 1.14 |

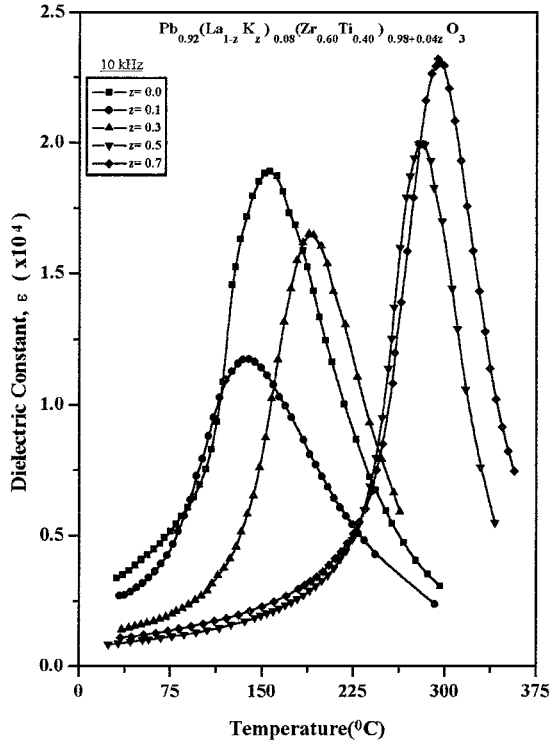


*Figure 4* Variation of dielectric constant ($\varepsilon$) of PLKZT with temperature at $10^4$ Hz.

temperature. A similar observation was made in the PLZT (8/65/35) compounds with different concentration of $K^+$ ions [12].

Fig. 2 shows transmission electron micrographs (TEM) and corresponding selected area electron diffraction (SAED) patterns (inset) of the calcined PLKZT powders. The interplanar spacings (d) observed from SAED and XRD are very much comparable (Table II). This confirms the presence of crystalline phase in the materials. It is also observed from TEM that the particles of PLKZT powders produced were spherical. It can be seen that the particles are well dispersed and the average particle size is about ~120 Å. However, the larger particles ≥150 Å showed some agglomeration [13].

Fig. 3 shows scanning electron micrographs (SEM) of sintered PLKZT pellets. The grains are nearly spherical.The average grain size (Table I) is uniform and the size distribution is quite narrow.

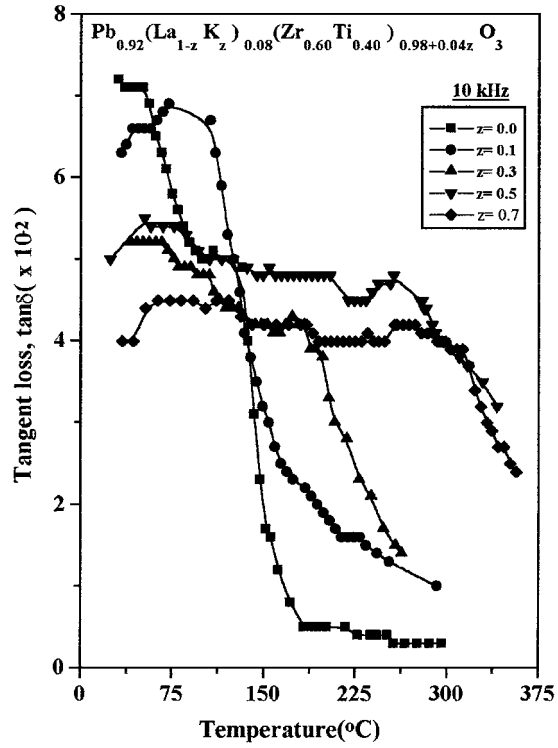


*Figure 5* Variation of tangent loss (tan $\delta$) of PLKZT with temperature at $10^4$ Hz.

Figs 4 and 5 show the variation of $\varepsilon$ and tan $\delta$ with temperature at $10^4$ Hz for all the compositions. Here the dielectric peak is broadened. This broadening of the dielectric peak and variation of $\varepsilon_{max}$ can be attributed to the variation of grain sizes and structural disorder [14] in the arrangement of the cations at the A-site (occupied by $Pb^{2+}$ along with $La^{3+}$ and $K^+$ additives), and/or at the B-site (occupied by $Zr^{4+}$ with lattice site vacancies). This leads to microscopic heterogeneity in the composition and a distribution of different local Curie points. In order to determine the degree of diffuseness in the materials the following expression was used [15]: $(1/\varepsilon - 1/\varepsilon_{max}) \propto (T - T_c)^\gamma$, where $\varepsilon$ is dielectric constant at temperature $T$ and $\varepsilon_{max}$ is its maximum value at $T_c$. The values of $\gamma$ (diffusivity) calculated from the graphs of $\ln(1/\varepsilon - 1/\varepsilon_{max})$ vs. $\ln(T - T_c)$ were found to be between 1 (for normal ferroelectrics) and 2 (completely disordered ferroelectrics), which confirm the diffuse phase transition in the materials. The value of maximum dielectric constant ($\varepsilon_{max}$) increases with the increasing doping concentration of $K^+$, which implies that addition of $K^+$ increases the dipole moment of the lattice [16]. The reciprocal dielectric constant is a linear function of temperature below and above $T_c$ except within the range of $\pm 20^\circ C$ around it. Moreover, the temperature gradient of the reciprocal dielectric constant in the ferroelectric and paraelectric phase is about 2 : 1 indicating the phase transition is of second order [14]. The ac electrical conductivity $\sigma$ is related to the dielectric constant, loss and temperature by the expressions: $\sigma = \omega\ \varepsilon\ \varepsilon_0$ tan $\delta$ and $\sigma = \sigma_0 \exp(-E_a/K_B T)$, where $\varepsilon_o$ is the dielectric constant at free space; $\omega$ is the angular frequency, $K_B$ is the Boltzmann constant and $E_a$ is the activation energy. Activation energy has been calculated from the plots of $\ln \sigma$ vs. $10^3/T$ in the

paraelectric region. The values of activation energy of the compounds are given in Table III.

The room temperature hysteresis loops of PLKZT are shown in Fig. 6. High electric field ($\sim$20–25 kV $\cdot$ cm$^{-1}$) was required to obtain saturation polarisation. The remanent polarisation ($P_r$) and coercive field ($E_c$) were determined from the hysteresis loop. It was observed that the hysteresis loop at 30°C for $z = 0.0$–0.5 is memory type. It becomes linear type with high coercivity for $z = 0.7$, which, may be due to the higher tetragonality in the compound [17]. The temperature dependence of $P_r$ of the materials are shown in Fig. 7. It has been observed that the polarisation appears to be quadratic, which again indicates a second order phase transition at $T_c$ [18]. The values of $E_c$ and $P_r$ at 30°C are given in Table III.

The variation of the $p^T$ of PLKZT with temperature is shown in Fig. 8. The transition temperature of the materials obtained from the pyroelectric measurement (Table III) is in good agreement with that obtained from dielectric and polarisation studies.

It has been observed that the piezoelectric strain coefficient ($d_{33}$) of PLKZT decreases with increase of $K^+$ concentration. The values of electromechanical coupling coefficients ($k_p, k_{31}$), frequency constant (FC) and mechanical quality factor ($Q_m$) are listed in Table III.

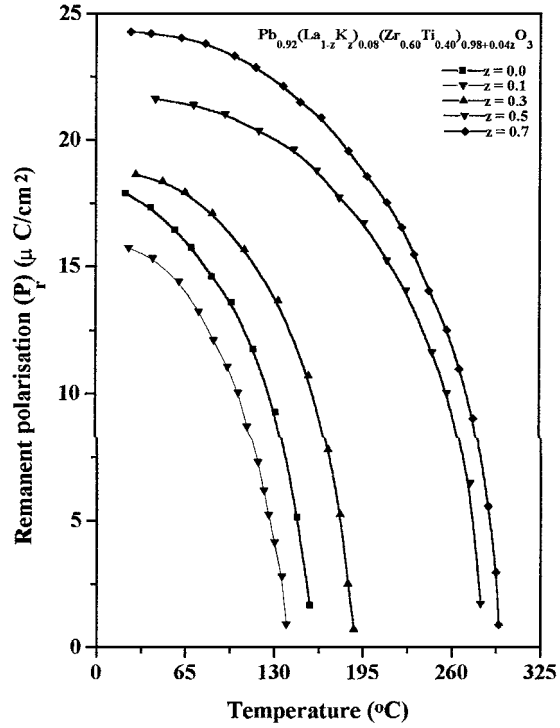


*Figure 7* Temperature dependence of remanent polarization ($P_r$) of PLKZT at 50 Hz.

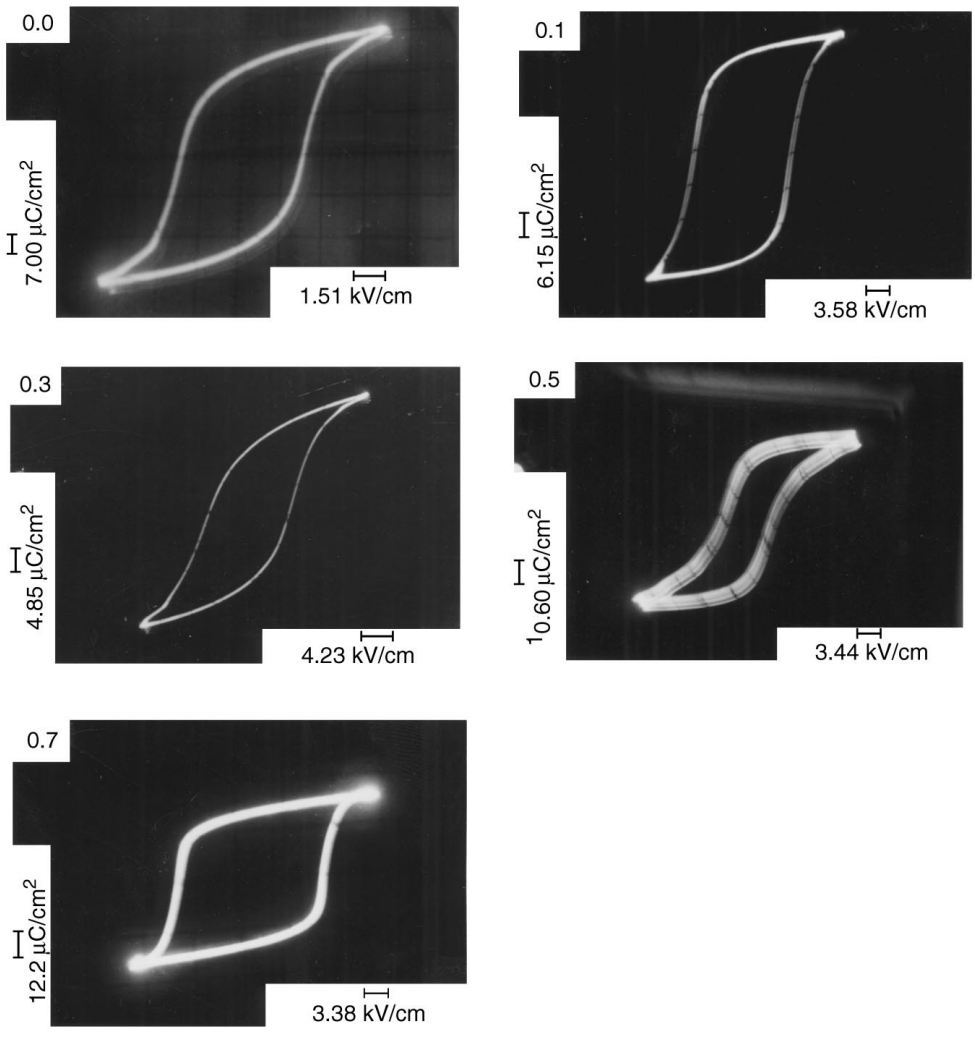


*Figure 6* Room temperature P-E hysteresis loop of PLKZT at 50 Hz.

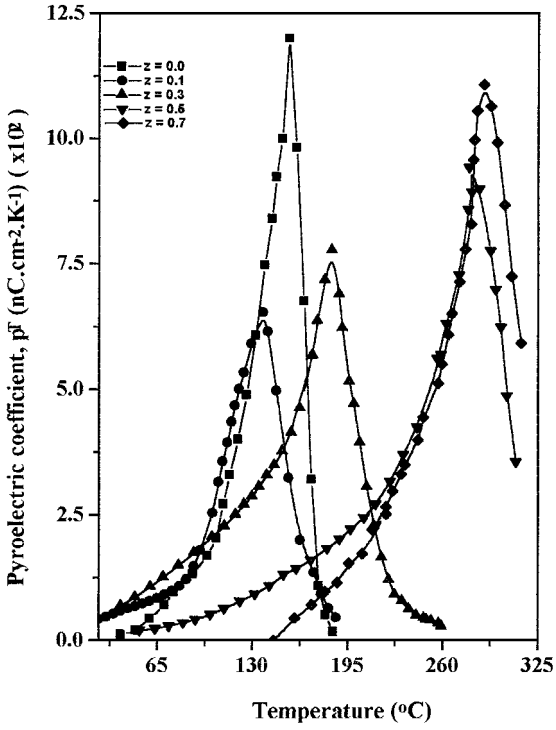


*Figure 8* Temperature dependence of pyroelectric coefficient ($p^T$) of PLKZT.

## 4. Conclusions

The sol-gel prepared PLKZT ceramics were found to be very fine and homogeneous. The interplanar spacing of the materials calculated from TEM and XRD were found to be very much comparable. The particles appear to be spherical. The grain size increases with the increase of doping concentration of $K^+$. The transition temperature, dielectric constant, $P_r$ and $E_c$ increase and $Q_m$ decreases with the increase of $K^+$ concentration. So a composition of donar and acceptor doped PZT materials leads to a stable ferroelectric state over a wide range.


## Acknowledgements

We are grateful to Prof. D. C. Agarwal, of IIT Kanpur for providing his laboratory facilities for piezoelectric measurements.


## References


1. B. JAFFE, R. S. ROTH and S. MARZULLO, *J. Appl. Phys.* **25** (1954) 909.
2. *Idem., J. Res. Nat. Bur. Stand.* **55** (1955) 239.
3. S. MIGA and K. WOJCIK, *Ferroelectrics* **100** (1989) 167.
4. K. L. YADAV, R. N. P. CHOUDHARY and T. K. CHAKI, *J. Mat. Sc.* **27** (1992) 5244.
5. K. L. YADAV and R. N. P. CHOUDHARY, *ibid.* **28** (1993) 769.
6. B. JAFFE, W. R. COOK and H. JAFFE, "Piezoelectric Ceramics" (Academic Press, New York, 1971) p. 148.
7. P. ROYCHOUDHARY and S. B. DESHPANDE, *Ind. J. Pure & Appl. Phys* **22** (1984) 708.
8. S.-L. FU, S. -Y. CHENG and C.-C. WEI, *Ferroelectrics* **67** (1986) 93.
9. R. LAL, S. C. SHARMA and R. DAYAL, *ibid.* **100** (1989) 43.
10. K. V. RAMANA MURTY, S. NARAYAN MURTY, K. UMAKANTHAM, A. BHANUMATI and K. LINGAMURTY, *ibid.* **119** (1991) 119.
11. Y. MASUDA, *ibid.* **63** (1985) 261.
12. K. L. YADAV and R. N. P. CHOUDHARY, *Mat. Lett.* **16** (1993) 291.
13. M. A. AKBAS and W. E. LEE, *Br. Ceram. Trans.* **95** (1996) 49.
14. M. E. LINES and A. M. GLASS, "Principles and applications of ferroelectrics and related materials" (Oxford Univ. Press, Oxford, 1977).
15. S. M. PILGRIM, A. E. SUTHERLAND and S. R. WINZER, *J. Amer. Ceram. Soc.* **73** (1990) 3122.
16. C. P. SMYTH, "Dielectric Behaviour and Structure" (McGraw Hill, New York, 1955).
17. A. J. MOULSON and J. M. HERBET, "Electroceramics" (Chapman and Hall, 1990) p. 358.
18. W. EYSEL, R. W. WOLFE and R. E. NEWNHAM, *J. Amer. Ceram. Soc.* **56** (1972) 185.



*Received 27 July 1998*
*and accepted 8 April 1999*